Invasions of European Tribes During Severe Cold Winters of the Past Three Millennia

Chuan-Chou Shen (river@ntu.edu.tw)
National Taiwan University
Hsun-Ming Hu
National Taiwan University
Wei Chen
Rastislav Milovský
Monika Orvošová
Ľubica Mareková
Demény Attila
Ryuji Asami
Horng-Sheng Mii
National Taiwan Normal University https://orcid.org/0000-0002-0702-3307
Yu-Tang Chien
Hideko Takayanagi
Yasufumi Iryu
https://orcid.org/0000-0002-6099-0662
Christoph Spötl
University of Innsbruck https://orcid.org/0000-0001-7167-4940

Article

Keywords:

Posted Date: March 28th, 2022

DOI: https://doi.org/10.21203/rs.3.rs-1463772/v1

Abstract

Times of turmoil in Europe during past millennia have been linked to hydroclimate variability. The invasion of foreign peoples that hastened the collapse of the Roman Empire, for example, was suggested to have been triggered by precipitation minima. However, the climate evolution of central-east Europe, the cradle of these tribes, remains elusive, thus limiting our understanding of how ancient civilizations responded to climate change. In this study, we present a 3000-year-long winter temperature and precipitation record inferred from a stalagmite in central Slovakia with dating uncertainties as small as ±6 yr. The data reveal that this region experienced seven 100-200 year-long cold intervals during the past three millennia. Three of these intervals with wet winters centered at 350 BC, and 400 and 900 AD coincided with historic invasion events in eastern Europe. These cold intervals were likely triggered by a weakened North Atlantic circulation and concomitant atmospheric blockings over western Europe.

Introduction

Climate-induced migration and the issue of climate refugees are particularly of concern in global climate governance. In the past, abrupt hydroclimatic changes or frequent occurrences of droughts/floods led to turmoil periods in human history (Meier et al., 2007; Sosnowski et al., 2016; Zhang et al., 2008; Büntgen et al., 2011). As a cradle of the ancient cultures, Europe featured several episodes of climate deterioration over the past millennia, which have been discussed as triggers of diseases (Appleby, 1980), population decrease (Patterson et al., 2010), and migrations (Thompson et al., 1999). Tribal invasions, especially the Great Migration in the 4^{th} to the 6^{th} century AD, profoundly affected European history. Studies over the past decades (Thompson et al., 1999; Wolfram, 1988; Goffart, 2006; Heather, 2010; Büntgen et al., 2011) hint towards a clear role of climate in triggering the movement of ancient tribes.

Tree-ring based late spring (April-June) precipitation records document high rainfall in central Europe during the Great Migration (Büntgen et al., 2011). However, Drake (2017) argued that the period of the Great Migration was instead characterized by a cold/dry climate, which played an important role in triggering the Great Migration. The conflict aspects of how climate influenced civilizations can be attributed to the spatial hydroclimate variability in Europe and the associated seasonal bias (e.g., Ortega et al., 2015). Paleoclimate proxy records, for example, can reflect only regional/seasonal hydroclimate conditions and result in an incomplete climatic understanding. To better investigate the relations between climate patterns and European invasion histories, precise and high-resolved paleoclimate records from the regions where the invaders originated are needed.

Here, we present a multi-proxy stalagmite record from central Slovakia, a region close to the cradle of the tribal invaders (Heather, 2010), which allows to decipher the winter temperature and precipitation changes over the last three thousand years. Our results show that three major invasion periods in Europe, including the Great Migration, coincide with anomalously cold winters in Slovakia, but not necessarily with droughts. These three events are the Celtic invasion during the 4^{th}-2^{nd} century BC, the Great Migration in the 4^{th}-6^{th} century AD, and the invasion of the Magyars during the 9^{th}-11^{th} century AD (Heather, 2010), all

of which originated in central-eastern Europe (Fig. 1; Supplementary Text). The 1:1 coincidence between the timing of these migrations and periods of persistent cold winters highlights the role of persistently cold climate episodes in triggering crises for central-eastern European tribes.

Materials And Methods

Zlomiska cave (48°59’ N, 19°40’ E, 809 m above sea level, a.s.l.) is 10.7 km in length and located within the Jánska dolina national nature reserve, Slovakia, in the northern part of Low Tatra Mountains (Fig. 1). The original cave entrance was a 0.5 m-wide crack in the ground which has been artificially enlarged. The region is characterized by a humid continental climate, with a mean annual temperature of 7.4 ˚C and a mean annual precipitation of 640 mm (1992-2016 AD) measured at the Global Network of Isotopes in Precipitation (GNIP) station at Liptovský Mikuláš Ondrašová (LMO; 49˚6' N, 19˚36' E, 570 m a.s.l.), 12 km north from Zlomiska cave.

A 28 cm-long stalagmite, ZL01, was collected in 2016 (Fig. S1) and the top 8 cm of this calcitic stalagmite was used in this study (Fig. S1). The chronology of this segment is based on U-Th ages with 2-sigma precision as good as ±6 yr (Shen et al., 2012; Cheng et al., 2013) (Methods S1) and the age model was constructed using StalAge (Scholz et al., 2011) (Fig. S2; Data S1). About 800 and 200 powdered subsamples were measured for $\delta^{18}O$ (Methods S2) and Sr/Ca and Ba/Ca, respectively (Methods S3). Hendy tests (Hendy, 1971) show that the δ18O variability along four growth layers is ± 0.03-0.11‰ (1-sigma) (Fig. S3), smaller than the instrumental 1-sigma external uncertainty of ± 0.12‰, suggesting insignificant kinetic isotope effects during calcite precipitation.

Results

3.1. The Zlomiska record

The studied section of ZL01 covers 1050 ± 35 BC to 1940 ± 11 AD. The ZL01 $\delta^{18}O$ values vary from −7.2 to −6.1‰ over past three thousand years (Fig. 2A) and feature seven centennial-scale negative excursions centered at 900, 600, 350, 100 BC, and 400, 900, 1500 AD. The Sr/Ca and Ba/Ca ratios range from 0.14-0.23 mmol/mol and 356-469 μmmol/mol, respectively (Fig. 2B). In general, Sr/Ca and Ba/Ca show relative high values before 1050 AD and decrease afterwards, reaching the minimum in the 1900s AD.

3.2. Seasonality of stalagmite proxies

In central Slovakia, strong evaporation in summer limits infiltration of rainfall (Wackerbarth et al. 2010), although over 60% of the annual precipitation falls between June and August. By subtracting potential evaporation (calculated using Thornthwaite 1948; Methods S4) from average precipitation (1992-2016 AD), effective infiltration at Zlomiska cave likely occurs only between October and March (Fig. S4), consistent with previous studies (Wackerbarth et al. 2010; Baker et al., 2019). This seasonal bias is supported by karst water data from Demänovská dolina cave system, 7 km west of Zlomiska cave,

whose mean $\delta^{18}O$ value of −10.8‰) (2010-2011 AD; Malík et al., 2012) is significantly lower than the long-term weighted mean rainwater $\delta^{18}O$ value of −9.4‰ (1992-2016 AD). This suggests that October-March precipitation with a mean $\delta^{18}O$ value of −13.2‰ (1992-2016 AD) is the main contribution to infiltration as opposed to summer (June-August) rain averaging −6.9‰. Accordingly, the ZL01 proxy records mainly reflect late autumn to early spring conditions (October-March; Baker et al., 2019).

3.3. ZL01 $\delta^{18}O$

Stalagmite $\delta^{18}O$ values, if depositing close to isotopic equilibrium, reflect the precipitation $\delta^{18}O$ value ($\delta^{18}O_p$) (Wackerbarth et al. 2010; Baker et al., 2019), which is governed by changes in air temperature, moisture source, and/or rainfall amount. The average monthly temperature at Zlomiska cave between October and March varies from −2 to 3 ˚C (1992-2016 AD) with a mean of 0.8 ˚C and a standard deviation of ±1.4 ˚C. An increase of 1 ˚C would result in a ~ −0.22‰ shift in stalagmite $\delta^{18}O$ due to the temperature-dependent isotope fractionation (O'Neil et al., 1969). The relationship between modern air temperature and $\delta^{18}O_p$ of 0.55±0.11 ‰/˚C (October-March; Fig. S5A) suggests that a temperature increase of 1 ˚C results in an increase of 0.55‰ in $\delta^{18}O_p$. Taken together, ±1 ˚C of temperature change results in ±0.33‰ of $\delta^{18}O_p$. The net temperature effect on stalagmite $\delta^{18}O$ is therefore ~0.33‰/˚C.

Changes of the relative proportion of moisture sourced from the Atlantic Ocean with $\delta^{18}O$ values of 0-0.5‰ and the Mediterranean Sea with higher $\delta^{18}O$ values of 1.0–1.5‰ can affect $\delta^{18}O_p$. The d-excess of moisture originating from the Atlantic Ocean (~10‰, Craig, 1961) is much lower than from the Mediterranean Sea (~22‰, Giustini, 2016). The absence of a significant correlation between d-excess and $\delta^{18}O_p$ (Fig. S5B) indicates that $\delta^{18}O_p$ in the study area does not reflect changes in moisture sources. LMO station data also show an insignificant correlation between precipitation amount and $\delta 18O_p$ (1992-2016 AD, October-March, Fig. S5C) showing that the amount effect does not play a role in this region.

These analyses show that the ZL01 $\delta^{18}O$ values are mainly governed by temperature, with negative (positive) stalagmite $\delta^{18}O$ values reflecting low (high) air temperatures (October-March), supported by stalagmites from caves in the Alps west of the study area (e.g., Boch et al., 2011; Meyer et al., 2008; Scholz et al., 2012). This temperature effect could be amplified by heavy snowfalls in colder winters that lead to a higher snowmelt contribution of isotopically depleted water to the cave dripwater in late spring (Lachniet, 2009; Unnikrishna et al., 2002). This argument can further be corroborated with the high degree of similarity between ZL01 $\delta^{18}O$ and temperature records from Tatry station (Slovakia; 49˚4’N, 20˚14’E, 694 m a.s.l.), Vienna station (Austria; 48˚13’N, 16˚21’E, 199 m a.s.l), and Praha-Klementinum (Czech Republic; 50˚05’N, 14˚25’E, 191 m a.s.l) (Fig. 3D). During the Roman Warm Period (RWP, ca. 250 BC to 350 AD) and the Medieval Climate Anomaly (MCA, ca. 950-1250 AD), high ZL01 $\delta^{18}O$ values suggest a warm winter climate (Fig. 2A); while during the Little Ice Age (LIA, ca. 1400-1850 AD), the low ZL01 $\delta^{18}O$ values indicate the opposite (Fig. 2A). Temperature variations at Tatry and Praha-Klementinum are closely related to Eastern European temperature changes (Fig. S6 A and B). Comparisons between ZL01 $\delta^{18}O$

and lower resolved winter temperature records from central-eastern Europe (Fig. S6C-F; Kaufman et al., 2020; Litt et al., 2009) also reveal a general consistency. These observations suggest that cold winters occurred across Eastern Europe and support that ZL01 $\delta^{18}O$ is a reliable qualitative proxy for regional October-March temperature.

3.4. ZL01 Sr/Ca and Ba/Ca

ZL01 Sr/Ca and Ba/Ca co-vary on a centennial scale over the past 3000 years. The high correlation between the two ratios (r = 0.87, n = 193, p < 0.05) points towards significant prior calcite precipitation (PCP) (Fairchild and McMillan 2007; Day and Henderson, 2013; Wassenburg et al., 2016, 2020). During dry conditions, the long residence time of drip water favors PCP and leads to high Sr/Ca and Ba/Ca ratios in the dripwater (Fairchild and McMillan 2007). Sr/Ca and Ba/Ca can thus be considered as precipitation proxies, with high Sr/Ca and Ba/Ca values corresponding to a dry climate, and *vice versa*.

Discussion

4.1. Regional temperature change and mechanism

The climate in Europe is strongly governed by the westerly winds which transport relative cool (warm) air masses from the Atlantic in summer (winter). In Slovakia, the North Atlantic Oscillation (NAO), with its positive (negative) phase associated with an increased (decreased) strength contrast of the Icelandic Low (IL) and the Azores High (AH), controls the westerly variability during October-March (Hurrell, 1995) and hence the temperature at the study site. The East Atlantic (EA) pattern (Barnston and Livezey, 1987) with its positive (negative) phase corresponding to a low (high) pressure anomaly in western Europe (centered at 55˚N and 20˚W), can also influence the position of the IL and the AH and the associated westerly routes. The October-March temperature at the Tatry meteorological station (1950-2012 AD) shows a strong correlation with sea-level pressure (SLP) anomalies at 60˚N and 10˚W (Fig. 3A, shades), resembling the correlation between the EA index (data from the Climate Prediction Center) and SLP (Fig. 3A, contours). The dipole correlation regions in the subtropics and the subpolar realm are also similar to the NAO pattern. The Tatry temperature time series (October-March) reveals some similarity to the NAO index (Fig. 3B; r = 0.31, n = 0.62, p < 0.05, 1950-2012; Jones et al., 1997) and the EA index (Fig. 3C; r = 0.41, n = 62, p < 0.01, 1950-2012; data from the Climate Prediction Center), corroborating that the NAO and EA modes both control October-March temperature at Zlomiska cave.

A negative (positive) NAO with reduced (enhanced) contrast between the IL and the AH lead to weak (strong) westerlies and less (more) warm air masses reaching the study area (Woollings et al., 2012). A negative (positive) EA, with a high (low) pressure anomaly over western Europe, reflects an increase (decrease) in atmospheric blocking frequency, which prevents (enables) the westerly winds to enter mainland Europe (Woollings et al., 2012; Madonna et al., 2017). The similarities between the ZL01 $\delta^{18}O$ record and instrumental NAO and EA indexes (Mellado-Cano et al., 2019; Comas-Bru and Hernández, 2018) back to 1685 AD (Fig. 3E and F) further confirm that the NAO and EA are important drivers of

temperature changes in the study area on multi-decadal to centennial time scales. The three multi-centennial cold periods registered by the minima in the ZL01 $\delta^{18}O$ record (Fig. 2A) could hence reflect weak or absent westerly winds.

Correlation analysis between the EA index and European precipitation (Fig. 4A) shows that a low (high) EA index, with a high (low) frequency of atmosphere blocking over western Europe, can lead to a dry (wet) climate on the British Isles and western/central Europe. Periods of cold winters inferred from the ZL01 $\delta^{18}O$ record match those with a dry climate inferred from low peat water-levels in Britain (Fig. 4B; Charman, 2010), high stalagmite Mg/Ca ratios in Bunker cave, NW Germany (Fig. 4C; Fohlmeister et al., 2012), high stalagmite growth rate in Roaring cave, Scotland (Fig. S8A; Baker et al., 2015), high Mg values (Fig. S8B) and high $\delta^{18}O$ values in stalagmites of Herbstlabyrith cave, central Germany (Waltgenbach et al., 2021) (Fig. S8C). The dry periods could have been also affected by a negative NAO phase, which impacts precipitation on the British Isles (Charman, 2010) and in Germany (Fohlmeister et al., 2012) (Fig. S9). The coherency between the ZL01 $\delta^{18}O$ time series and proxy records from Britain and Germany suggests that, during the intervals of ZL01 $\delta^{18}O$ minima, weak westerlies resulted in reduced moisture transport to the British Isles and western Europe and low temperatures in Slovakia. This climate pattern likely resulted from strong atmospheric blockings over western Europe, similar to a negative EA or NAO phase.

4.2. Climate change and tribal migrations

The periods of three main tribal invasions into Europe, the Celtic invasion (ca. 4^{th}-2^{nd} century BC), the Great Migration (ca. 4^{th}-6^{th} century AD), and the invasion of the Magyars (ca. 9^{th}-11^{th} century AD) coincide with distinct intervals of anomalously cold winters as inferred from the ZL01 $\delta^{18}O$ record (Figs. 2A), suggesting a possible link between of human migrations and climate. Severe cold winters are known to delay germination, lower the resistance to diseases, and reduce the yield and quality of crops (Hussain et al. 2018; Liu et al., 2020), eventually forcing humans to migrate. ZL01 Sr/Ca and Ba/Ca records suggest humid conditions during the Celtic invasion, the Great Migration, and the invasion of the Magyars (Fig. 2B). These data argue against the hypothesis of the drought-driven migrations (e.g., Drake, 2017) and instead emphasize the importance of temperature changes on human activities in central-east Europe. In addition to anomalously cold winters, low summer temperatures as recorded by tree-ring data (Büntgen et al. 2011) (Fig. S7) could also be mportant in triggering these tribal movements.

In central-eastern Europe, variations in the intensity of the westerlies might have had less impact on precipitation compared to temperature, as the atmospheric moisture decreases along the westerly tracks from the Atlantic Ocean. This is supported by the lack of a correlation between the NAO index and precipitation amount in the study area (Fig. S9). Accordingly, changes in the orientation and intensity of the westerlies led to temperature rather than precipitation changes in central-eastern Europe, different from the northern fringe of the Mediterranean Sea, which is more sensitive to hydroclimate changes (e.g., Cullen et al., 2000; Drysdale et al., 2006).

4.3. Possible mechanism

Cold periods with enhanced blockings over western Europe on decadal to centennial time scales suggest that the positions of the AH and the IL shifted towards high latitudes (Moore et al., 2013; Comas-Bru and Mcdermott, 2014). This poleward displacement of the AH and the IL was suggested to be induced by cooling of the high-latitude Atlantic Ocean, which shifts the region of transient eddy heat flux at 850 hPa northward (Rivière, 2009; Kown et al., 2020). This hypothesis is supported by the coherency between the ZL01 $\delta^{18}O$ record and sea-surface temperatures (SST) along the path of the North Atlantic Current (Saenger et al., 2011) (Fig. S10B), with low SSTs corresponding to a weakened warm water transport from the tropical Atlantic to the polar region. Minima in ZL01 $\delta^{18}O$ data are also in accordance with periods of weak Atlantic Multidecadal Variability (AMV) (Lapointe et al., 2020) (Fig. S10C). This suggests that a weak Atlantic Meridional Ocean Circulation (AMOC) reduces warm water transport from the equator to the polar regions, in turn leading to a cooling of the North Atlantic.

The NAO could also affect the (winter) temperature in the study area, but periods of $\delta^{18}O$ minima are unrelated to negative NAO phases (Fig. S11) (Olsen et al., 2012; Ortega et al., 2015), possibly because (*i*) the NAO phase change was not the dominate forcing during the past three millennia in this region, and/or (*ii*) limitations of NAO reconstructions (Ortega et al., 2015) hamper such a comparison. Finally, intervals of high volcanic activity (Fig. S10A; Kobashi et al., 2017) show no relationship with minima in ZL01 $\delta^{18}O$, arguing against a volcanic forcing of these cold intervals.

Conclusion

Previous studies showed that the Great Migration during the late Roman Empire might have been triggered by prolonged dry conditions (e.g., Drake, 2017). Our 3000 yr-long $\delta^{18}O$ and trace elemental record from Slovakia shows that this tribal invasion event during the 4^{th}-6^{th} century AD and two other migrations in the 4^{th}-2^{nd} century BC and the 9^{th}-11^{th} century AD coincide with centennial-scale cool periods rather than droughts (Fig. 2). These cool periods could be triggered by a weak AMOC that induced atmospheric blockings over western Europe and prevented the transport of relatively warm wintertime air masses to central Europe.

Declarations

Acknowledgments: We are thankful for the financial support provided by grants from the Science Vanguard Research Program of the Ministry of Science and Technology (MOST) (110-2123-M-002-009), the National Taiwan University (109L8926 to C.-C.S.), the Higher Education Sprout Project of the Ministry of Education (110L901001 and 110L8907).

Author contributions: C.-C.S. directed this research. C.-C.S., H.-M.H., and W.C. conceived the project. C.-C.S., H.-M.H., R.M. and L.L. conducted field surveys and collected the speleothem. H.-M.H, D.A., R.A. and H.-S.M. conducted sample preparation and isotope measurements. H.-M.H and W.C. performed U-Th

dating. H.-M.H, W.C. and C.S. prepared the draft and interpretations, and all authors contributed to manuscript completion.

Competing interests: Authors declare no competing interests.

References

1. Appleby, A. (1980). Epidemics and famine in the Little Ice Age. *Journal of Interdisciplinary History*, 10(4), 643-663.
2. Baker, A., C. Hellstrom, J., Kelly, B. F. J., Mariethoz, G., & Trouet, V. (2015). A composite annual-resolution stalagmite record of North Atlantic climate over the last three millennia. *Scientific Reports*, *5*, 10307. https://doi.org/10.1038/srep10307
3. Baker, A., Hartmann, A., Duan, W., Hankin, S., Comas-Bru, L., Cuthbert, M. O., Treble, P. C., Banner, J., Genty, D., Baldini, L. M., Bartolomé, M., Moreno, A., Pérez-Mejías, C., & Werner, M. (2019). Global analysis reveals climatic controls on the oxygen isotope composition of cave drip water. *Nature Communications*, *10*(1), 1–7. https://doi.org/10.1038/s41467-019-11027-w.
4. Barnston, A. G., & Livezey, R. E. (1987). Classification, seasonality and persistence of low-frequency atmospheric circulation patterns. *Monthly Weather Review*, *115*(6), 1083–1126. https://doi.org/10.1175/1520-0493.
5. Boch, R., Cheng, H., Spötl, C., Edwards, R. L., Wang, X., & Häuselmann, P. (2011). NALPS: A precisely dated European climate record 120-60 ka. *Climate of the Past* 7(4):1247–59. doi: 10.5194/cp-7-1247-2011.
6. Büntgen, U., Tegel, W., Nicolussi, K., McCormick, M., Frank, D., Trouet, V., Kaplan, J. O., Herzig, F., Heussner, K.-U., Wanner, H., Luterbacher, J., & Esper, J. (2011). 2500 years of European climate variability and human susceptibility. *Science*, 331, 578–582. https://doi.org/10.1126/science.1197175.
7. Charman, D. J. (2010). Centennial climate variability in the British Isles during the mid–late Holocene. *Quaternary Science Reviews*, *29*(13–14), 1539–1554. https://doi.org/10.1016/j.quascirev.2009.02.017
8. Comas-Bru, L., & McDermott, F. (2014). Impacts of the EA and SCA patterns on the European twentieth century NAO-winter climate relationship. *Quarterly Journal of the Royal Meteorological Society*, *140*, 354–363. https://doi.org/10.1002/qj.2158
9. Comas-Bru, L., & Hernández, A. (2018). Reconciling North Atlantic climate modes: Revised monthly indices for the East Atlantic and the Scandinavian patterns beyond the 20th century. *Earth System Science Data* 10(4):2329–44. doi: 10.5194/essd-10-2329-2018.
10. Craig, H. (1961). Isotopic variations in meteoric waters. *Science* 133:1702–3. doi: 10.1126/science.133.3465.1702.
11. Cheng, H., Edwards, R.L., Shen, C. C., Polyak, V. J., Asmerom, Y., Woodhead, J., Hellstrom, J., Wang, Y., Kong, X., Spötl, C., Wang, X., & Calvin Alexander, E. (2013). Improvements in ^{230}Th dating, ^{230}Th and

^{234}U half-life values, and U-Th isotopic measurements by multi-collector inductively coupled plasma mass spectrometry. *Earth and Planetary Science Letters*, *371–372*, 82–91. https://doi.org/10.1016/j.epsl.2013.04.006

12. Cullen, H. M., De Menocal, P. B., Hemming, S., Brown, F. H., Guilderson, T., & Sirocko, F. (2000). Climate change and the collapse of the Akkadian empire: Evidence from the deep sea. *Geology*, *28*(4), 379–382. https://doi.org/10.1130/0091-7613(2000)
13. Day, C. C., & Henderson, G. M. (2013). Controls on trace-element partitioning in cave-analogue calcite. *Geochimica et Cosmochimica Acta* 120:612–27. doi: 10.1016/j.gca.2013.05.044.
14. Drake, B. L. (2017). Changes in North Atlantic Oscillation drove population migrations and the collapse of the Western Roman Empire. *Scientific Reports* 7(1):1227. doi: 10.1038/s41598-017-01289-z.
15. Drysdale, R., Zanchetta, G., Hellstrom, J., Maas, R., Fallick, A., Pickett, M., Cartwright, I., & Piccini, L. (2006). Late Holocene drought responsible for the collapse of Old World civilizations is recorded in an Italian cave flowstone. *Geology*, *34*(2), 101. https://doi.org/10.1130/G22103.1
16. Fairchild, I. J., & McMillan, E. A. (2007). Speleothems as indicators of wet and dry periods. *International Journal of Speleology* 36(2):69–74. doi: 10.5038/1827-806X.36.2.2.
17. Fohlmeister, J., Schröder-Ritzrau, A., Scholz, D., Spötl, C., Riechelmann, D. F. C., Mudelsee, M., Wackerbarth, A., Gerdes, A., Riechelmann, S., Immenhauser, A., Richter, D. K., & Mangini, A. (2012). Bunker Cave stalagmites: An archive for central European Holocene climate variability. *Climate of the Past*, *8*(5), 1751–1764. https://doi.org/10.5194/cp-8-1751-2012
18. Giustini, F., Brilli, M., & Patera, A. (2016). Mapping oxygen stable isotopes of precipitation in Italy. *Journal of Hydrology: Regional Studies* 8:162–81. doi: 10.1016/j.ejrh.2016.04.001.
19. Goffart, W. (2006). Barbarian tides: the migration age and the later Roman Empire. Philadelphia, PA: University of Pennsylvania Press.
20. Heather, P. (2010). Empires and barbarians: the fall of Rome and the birth of Europe. Oxford: Oxford University Press.
21. Hendy, C. (1971). The isotopic geochemistry of speleothems—I. The calculation of the effects of different modes of formation on the isotopic composition of speleothems and their applicability as palaeoclimatic indicators. *Geochimica et Cosmochimica Acta* 35(8):801–24. doi: 10.1016/0016-7037(71)90127-X.
22. Hurrell, J. W. (1995). Decadal trends in the North Atlantic Oscillation: Regional temperatures and precipitation. *Science* 269, 676–79. doi: 10.1126/science.269.5224.676.
23. Hussain, H. A., Hussain, S., Khaliq, A., Ashraf, U., Anjum, S. A., Men, S., & Wang, L. (2018). Chilling and drought stresses in crop plants: Implications, cross talk, and potential management opportunities. *Frontiers in Plant Science*, *9*, 1–21. https://doi.org/10.3389/fpls.2018.00393
24. Jones, P. D., Jonsson, T., & Wheeler, D. (1997). Extension to the North Atlantic Oscillation using early instrumental pressure observations from Gibraltar and south-west Iceland. *International Journal of Climatology*, *17*(13), 1433–1450.

25. Kaufman, D., McKay, N., Routson, C., Erb, M., Davis, B., Heiri, O., Jaccard, S., Tierney, J., Dätwyler, C., Axford, Y., Brussel, T., Cartapanis, O., Chase, B., Dawson, A., de Vernal, A., Engels, S., Jonkers, L., Marsicek, J., Moffa-Sánchez, P., … Zhilich, S. (2020). A global database of Holocene paleotemperature records. *Scientific Data*, *7*(1), 115. https://doi.org/10.1038/s41597-020-0445-3.
26. Kobashi, T., Menviel, L., Jeltsch-Thömmes, A., Vinther, B. M., Box, J. E., Muscheler, R., Nakaegawa, T., Pfister, P. L., Döring, M., Leuenberger, M., Wanner, H., & Ohmura, A. (2017). Volcanic influence on centennial to millennial Holocene Greenland temperature change. *Scientific Reports*, *7*(1), 1–10. https://doi.org/10.1038/s41598-017-01451-7
27. Kwon, Y. O., Seo, H., Ummenhofer, C. C., & Joyce, T. M. (2020). Impact of multidecadal variability in Atlantic SST on winter atmospheric blocking. *Journal of Climate*, *33*(3), 867–892. https://doi.org/10.1175/JCLI-D-19-0324.1
28. Lachniet, M. S. (2009). Climatic and environmental controls on speleothem oxygen-isotope values. *Quaternary Science Reviews* 28(5–6):412–32. doi: 10.1016/j.quascirev.2008.10.021.
29. Lapointe, F., Bradley, R. S., Francus, P., Balascio, N. L., Abbott, M. B., Stoner, J. S., St-Onge, G., de Coninck, A., & Labarre, T. (2020). Annually resolved Atlantic sea surface temperature variability over the past 2,900 y. *Proceedings of the National Academy of Sciences*, *117*(44), 27171–27178. https://doi.org/10.1073/pnas.2014166117
30. Litt, T., Schölzel, C., Kühl, N., & Brauer, A. (2009). Vegetation and climate history in the Westeifel Volcanic Field (Germany) during the past 11 000 years based on annually laminated lacustrine maar sediments. *Boreas*, *38*(4), 679–690. https://doi.org/10.1111/j.1502-3885.2009.00096.x
31. Liu, L., Xia, Y., Liu, B., Chang, C., Xiao, L., Shen, J., Tang, L., Cao, W., & Zhu, Y. (2020). Individual and combined effects of jointing and booting low-temperature stress on wheat yield. *European Journal of Agronomy*, *113*, 125989. https://doi.org/10.1016/j.eja.2019.125989
32. Madonna, E., Li, C., Grams, C. M., & Woollings, T. (2017). The link between eddy-driven jet variability and weather regimes in the North Atlantic-European sector. *Quarterly Journal of the Royal Meteorological Society* 143:2960–72. doi: 10.1002/qj.3155.
33. Malík, P., Mikita, S., Grolmusová, Z., & Michalko, J. (2012). Monitoring of hydrogen and oxygen isotopes of waters in the Demänovská dolina valley and its underground hydrologic system. 39th IAH Congress, Niagara Falls, Canada. https://doi.org/10.13140/2.1.4148.5762
34. Meier, P., Bond, D., & Bond, J. (2007). Environmental influences on pastoral conflict in the Horn of Africa. *Political Geography* 26(6):716–35. doi: https://doi.org/10.1016/j.polgeo.2007.06.001.
35. Mellado-Cano, J., Barriopedro, D., García-Herrera, R., Trigo, R. M., & Hernández, A. (2019). Examining the North Atlantic Oscillation, East Atlantic pattern, and jet variability since 1685. *Journal of Climate* 32(19):6285–98. doi: 10.1175/JCLI-D-19-0135.1.
36. Meyer, M. C., Spötl, C., & Mangini, A. (2008). The demise of the Last Interglacial recorded in isotopically dated speleothems from the Alps. *Quaternary Science Reviews* 27(5–6):476–96. doi: 10.1016/j.quascirev.2007.11.005.

37. Moore, G. W. K., Renfrew, I. A., & Pickart, R. S. (2013). Multidecadal mobility of the North Atlantic Oscillation. *Journal of Climate*, *26*(8), 2453–2466. https://doi.org/10.1175/JCLI-D-12-00023.1

38. O'Neil, J. R., Clayton, R. N., & Mayeda, T. K. (1969). Oxygen isotope fractionation in divalent metal carbonates. *Journal of Chemical Physics* 51(12):5547–58. doi: 10.1063/1.1671982.

39. Olsen, J., Anderson, N. J., & Knudsen, M. F. (2012). Variability of the North Atlantic Oscillation over the past 5,200 years. *Nature Geoscience*, *5*(11), 808–812. https://doi.org/10.1038/ngeo1589

40. Ortega, P., Lehner, F., Swingedouw, D., Masson-Delmotte, V., Raible, C. C., Casado, M., & Yiou, P. (2015). A model-tested North Atlantic Oscillation reconstruction for the past millennium. *Nature*, *523*, 71–74. https://doi.org/10.1038/nature14518.

41. Patterson, W. P., Dietrich, K. A., Holmden, C., & Andrews, J. T. (2010). Two millennia of North Atlantic seasonality and implications for Norse colonies. *Proceedings of the National Academy of Sciences* 107(12):5306–10. doi: 10.1073/pnas.0902522107.

42. Rivière, G. (2009). Effect of latitudinal variations in low-level baroclinicity on eddy life cycles and upper-tropospheric wave-breaking processes. *Journal of the Atmospheric Sciences*, *66*(6), 1569–1592. https://doi.org/10.1175/2008JAS2919.1

43. Saenger, C., Came, R. E., Oppo, D. W., Keigwin, L. D., & Cohen, A. L. (2011). Regional climate variability in the western subtropical North Atlantic during the past two millennia. *Paleoceanography*, *26*(2), 1–12. https://doi.org/10.1029/2010PA002038

44. Scholz, D., & Hoffmann, D. L. (2011). StalAge – An algorithm designed for construction of speleothem age models. *Quaternary Geochronology* 6(3):369–82. doi: https://doi.org/10.1016/j.quageo.2011.02.002.

45. Scholz, D., Frisia, S., Borsato, A., Spötl, C., Fohlmeister, J., Mudelsee, M., Miorandi, R., & Mangini, A. (2012). Holocene climate variability in north-eastern Italy: potential influence of the NAO and solar activity recorded by speleothem data. *Climate of the Past* 8(4):1367–83. doi: 10.5194/cp-8-1367-2012.

46. Shen, C.-C., Wu, C.-C., Cheng, H., Edwards, R.L., Hsieh, Y.-T., Gallet, S., Chang, C.-C., Li, T.-Y., Lam, D. D., Kano, A., Hori, M., & Spötl, C. (2012). High-precision and high-resolution carbonate ^{230}Th dating by MC-ICP-MS with SEM protocols. *Geochimica et Cosmochimica Acta*, *99*, 71–86. https://doi.org/10.1016/j.gca.2012.09.018

47. Sosnowski, A., Ghoneim, E., Burke, J. J., Hines, E., & Halls, J. (2016). Remote regions, remote data: A spatial investigation of precipitation, dynamic land covers, and conflict in the Sudd wetland of South Sudan. *Applied Geography* 69:51–64. doi: https://doi.org/10.1016/j.apgeog.2016.02.007.

48. Thompson, E., & Heather, P. (1999). The Huns. Oxford, England: Blackwell.

49. Thornthwaite, C. W. (1948). An approach toward a rational classification of climate. *Geographical Review* 38(1):55–94. doi: 10.2307/210739.

50. Unnikrishna, P. V., McDonnell, J. J., & Kendall, C. (2002). Isotope variations in a Sierra Nevada snowpack and their relation to meltwater. *Journal of Hydrology* 260(1–4):38–57. doi: 10.1016/S0022-1694(01)00596-0.

51. Waltgenbach, S., Riechelmann, D. F. C., Spötl, C., Jochum, K. P., Fohlmeister, J., Schröder-Ritzrau, A., & Scholz, D. (2021). Climate variability in central Europe during the last 2500 years reconstructed from four high-resolution multi-proxy speleothem records. *Geosciences*, *11*(4). https://doi.org/10.3390/geosciences11040166
52. Wassenburg, J. A., Scholz, D., Jochum, K. P., Cheng, H., Oster, J., Immenhauser, A., Richter, D. K., Häger, T., Jamieson, R. A., Baldini, J. U. L., Hoffmann, D., & Breitenbach, S. F. M. (2016). Determination of aragonite trace element distribution coefficients from speleothem calcite–aragonite transitions. *Geochimica et Cosmochimica Acta* 190:347–67. doi: 10.1016/j.gca.2016.06.036.
53. Wassenburg, J. A., Riechelmann, S., Schröder-Ritzrau, A., Riechelmann, D. F. C., Richter, D. K., Immenhauser, A., Terente, M., Constantin, S., Hachenberg, A., Hansen, M., & Scholz, D. (2020). Calcite Mg and Sr partition coefficients in cave environments: Implications for interpreting prior calcite precipitation in speleothems. *Geochimica et Cosmochimica Acta* 269:581–96. doi: https://doi.org/10.1016/j.gca.2019.11.011.
54. Wackerbarth, A., Scholz, D., Fohlmeister, J., & Mangini, A. (2010). Modelling the $\delta^{18}O$ value of cave drip water and speleothem calcite. *Earth and Planetary Science Letters* 299(3–4):387–97. doi: 10.1016/j.epsl.2010.09.019.
55. Wolfram, H. (1988). History of the Goths. Berkeley, CA: University of California Press.
56. Woollings, T., & Blackburn, M. (2012). The North Atlantic jet stream under climate change and its relation to the NAO and EA patterns. *Journal of Climate* 25(3):886–902. doi: 10.1175/JCLI-D-11-00087.1.
57. Zhang, P., Cheng, H., Edwards, R. L., Chen, F., Wang, Y., Yang, X., Liu, J. J., Tan, M., Wang, X., An, C., Dai, Z., Zhou, J., Zhang, D., Jia, J., Jin, L., & Johnson, K. R. (2008). A test of climate, sun, and culture relationships from an 1810-year Chinese cave record. *Science* 322:940–42. doi: 10.1126/science.1163965.

Figures

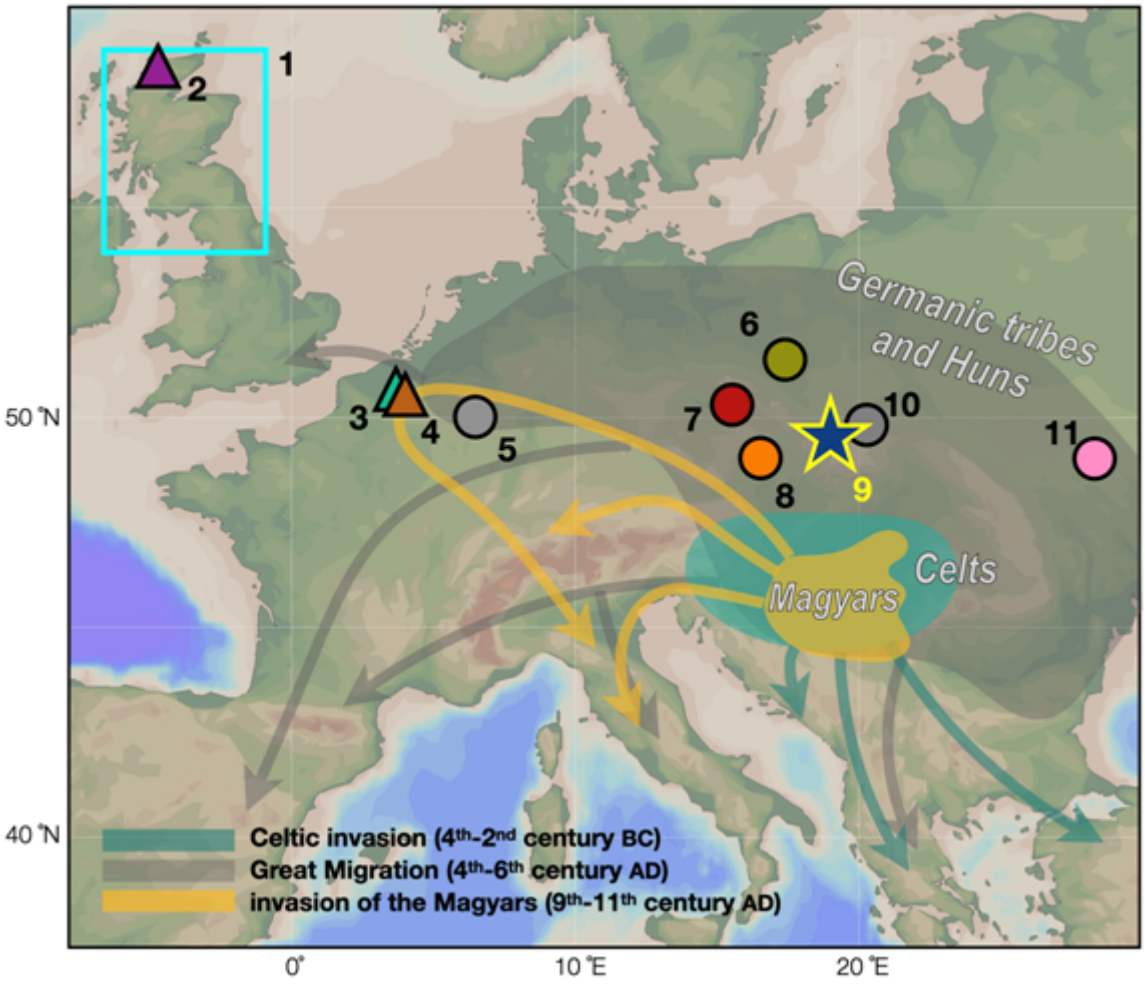

Figure 1

Map showing the locations of records and tribal migrations. The star marks Zlomiska cave. The triangle and circles denote caves and other sites with geological/instrumental records, respectively. 1. Stacked paleo-water table record from peat deposits on the British Isles (Charman et al., 2010). 2. Roaring cave (Baker et al., 2015). 3. Bunker cave (Fohlmeister et al., 2012). 4. Herbstlabyrinth cave (Waltgenbach et al., 2021) 5. Meerfelder Maar and Holzmaar (Litt et al., 2009). 6. Lake Lednica (Kaufman et al., 2020). 7. Praha-Klementinum meteorological station. 8. Vienna meteorological station. 9. Zlomiska cave (this study). 10. Tatry meteorological station. 11. Dovjok Swamp (Kaufman et al., 2020). The color-shaded areas and arrows show the origins and routes of tribal migrations (Heather, 2012). The map was generated using Ocean Data View.

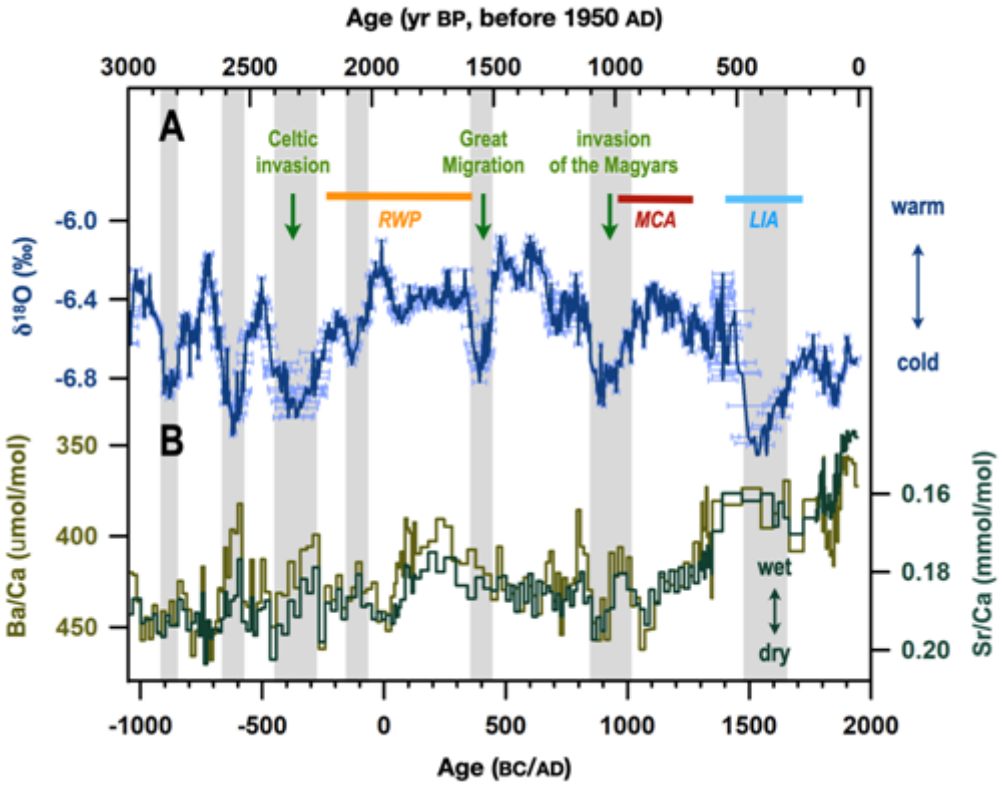

Figure 2

Proxy records of stalagmite ZL01 from Zlomiska cave. (A) $\delta^{18}O$ record. Error bars denote 2-sigma age uncertainties. **(B)** Ba/Ca (dark yellow) and Sr/Ca (dark green). Note inverted axes. Grey vertical bars denote seven 100-200 yr-long cold wintertime periods recorded by the $\delta^{18}O$ data. Horizontal bars denote the Roman Warm Period (RWP), the Medieval Climate Anomaly (MCA), and the Little Ice Age (LIA).

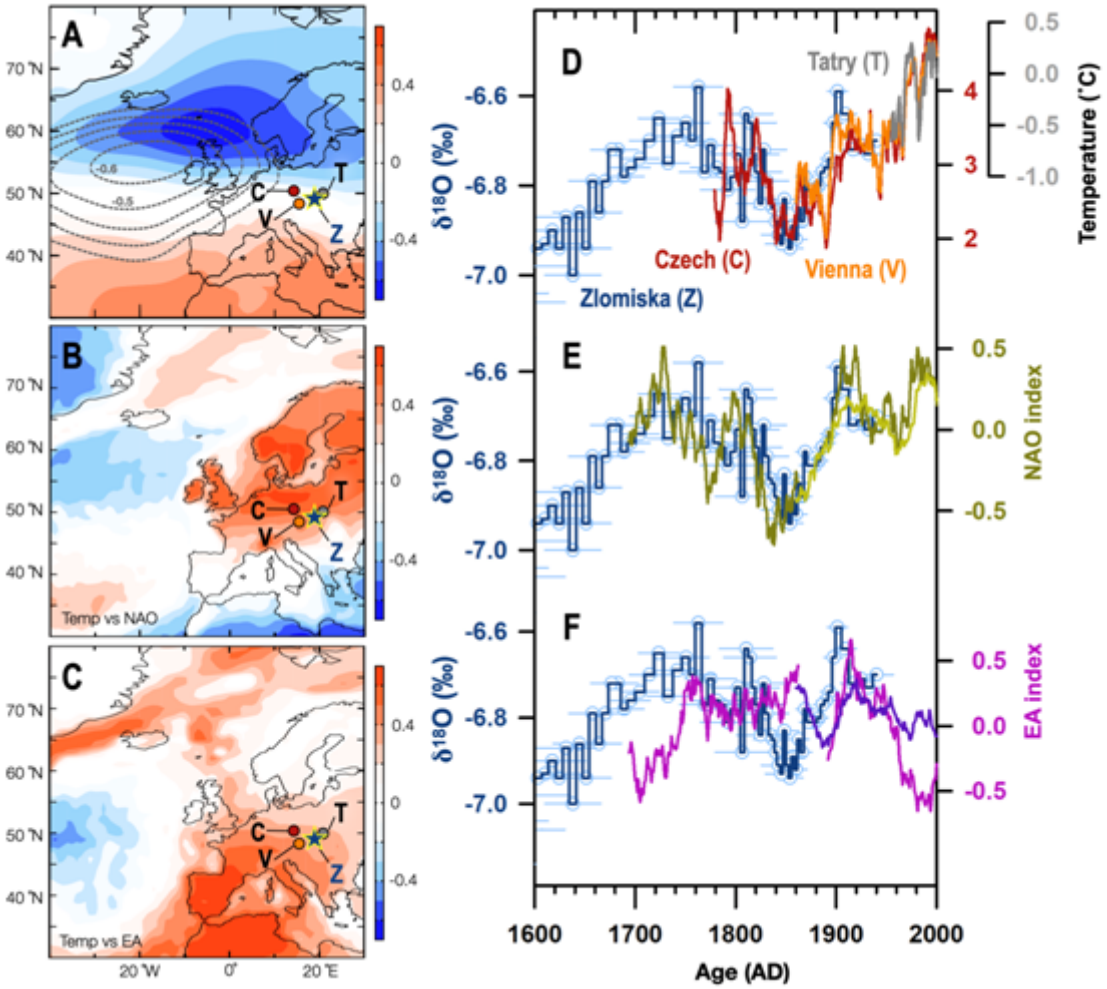

Figure 3

Modern climate and stalagmite ZL01 $\delta^{18}O$.(A) Correlation map between sea-level pressure (SLP) and Tatry temperature (shades)/EA index (contours), October-March 1950-2012 AD. **(B)** Correlation map between temperature and NAO index (October-March 1950-2012 AD). **(C)** As for **(B)** but for temperature and EA index (October-March 1950-2012 AD). Color shades in **(A)-(C)** are correlation coefficients above 90% confident level. NAO index and EA index used in **(A)-(C)** are from Jones et al. (1997) and the Climate Prediction Center (CPC). **(D)** ZL01 $\delta^{18}O$ (dark blue) and temperature records (10-yr running mean) from Tatry (T, grey), Vienna (V, orange) and Praha-Klementinum (C, dark red), October-March. The locations of these meteorological stations are shown in **(A)-(C)**. **(E)** ZL01 $\delta^{18}O$ (dark blue) and instrumentally based NAO index (20-yr running mean) from Comas-Bru et al. (2018) (light mustard) and Melledo-Cano et al. (2019) (mustard). **(F)** As **(E)**, but for the EA index (20-yr running mean) from Comas-Bru et al. (2018) (purple) and Melledo-Cano et al. (2019) (pink). Error bars in **(D)-(F)** denote 2-sigma age uncertainties. Temperature and SLP data are from 20th century Reanalysis v3.

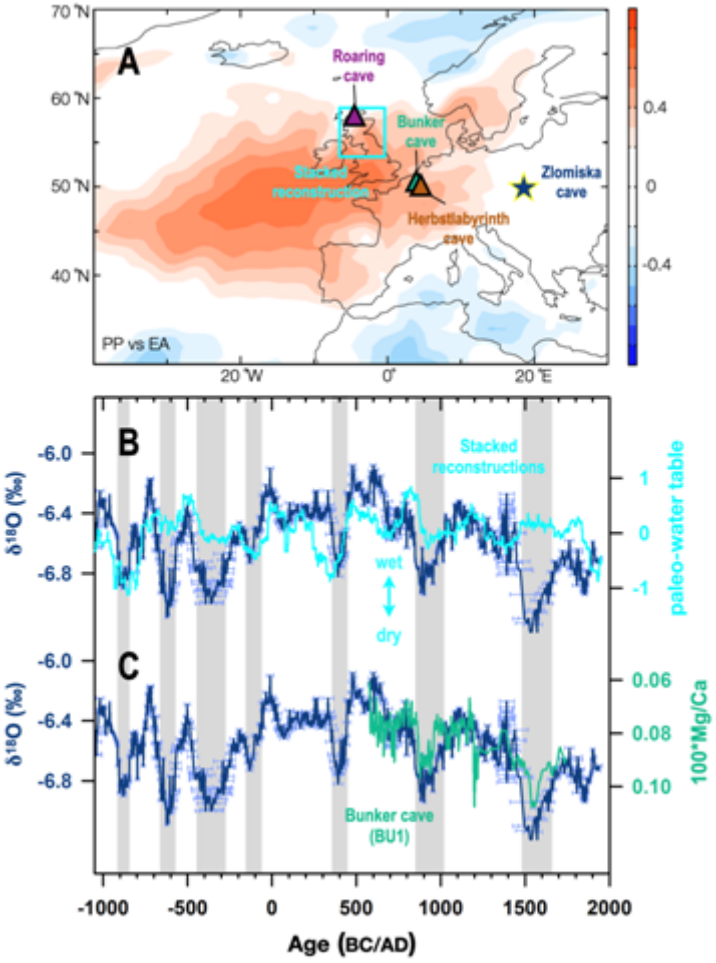

Figure 4

Atmospheric blocking and associated precipitation records. (A) Correlation map between precipitation and EA index (October-March 1950-2012 AD). Color shades are correlation coefficients above 90% confident level. Blue rectangle indicates the region where the stacked peat paleo-water table records were reconstructed. **(B)** ZL01 $\delta^{18}O$ (dark blue) and stacked reconstructions of peat paleo-water table (aqua; Charman et al., 2010). **(C)** ZL01 $\delta^{18}O$ (dark blue) and Bunker cave Mg/Ca ratios (green; Fohlmeister et al., 2012) as a precipitation proxy. Error bars in **(B)** and **(C)** denote 2-sigma age uncertainties. Grey vertical bars in **(B)** and **(C)** mark the seven centennial-scale cold wintertime periods inferred from ZL01 $\delta^{18}O$ data.

Supplementary Files

This is a list of supplementary files associated with this preprint. Click to download.

- DataS3SrCaandBaCaofZL01.xlsx
- DataS2XX18OofZL01.xlsx
- DataS1UThdatingresultsofZL01.xlsx

- 2022HusuppSlovakiav11.docx